Annals of Botany **112**: 1067–1081, 2013
doi:10.1093/aob/mct175, available online at www.aob.oxfordjournals.org

ANNALS OF BOTANY
Founded 1887

Early local differentiation of the cell wall matrix defines the contact sites in lobed mesophyll cells of *Zea mays*

E. Giannoutsou, P. Sotiriou, P. Apostolakos and B. Galatis*

Department of Botany, Faculty of Biology, University of Athens, Athens 15784, Greece
** For correspondence. E-mail bgalatis@biol.uoa.gr*

Received: 17 April 2013 Returned for revision: 20 May 2013 Accepted: 12 June 2013 Published electronically: 22 August 2013

• *Background and Aims* The morphogenesis of lobed mesophyll cells (MCs) is highly controlled and coupled with intercellular space formation. Cortical microtubule rings define the number and the position of MC isthmi. This work investigated early events of MC morphogenesis, especially the mechanism defining the position of contacts between MCs. The distributions of plasmodesmata, the hemicelluloses callose and (1 → 3,1 → 4)-β-D-glucans (MLGs) and the pectin epitopes recognized by the 2F4, JIM5, JIM7 and LM6 antibodies were studied in the cell walls of *Zea mays* MCs.
• *Methods* Matrix cell wall polysaccharides were immunolocalized in hand-made sections and in sections of material embedded in LR White resin. Callose was also localized using aniline blue in hand-made sections. Plasmodesmata distribution was examined by transmission electron microscopy.
• *Results* Before reorganization of the dispersed cortical microtubules into microtubule rings, particular bands of the longitudinal MC walls, where the MC contacts will form, locally differentiate by selective (1) deposition of callose and the pectin epitopes recognized by the 2F4, LM6, JIM5 and JIM7 antibodies, (2) degradation of MLGs and (3) formation of secondary plasmodesmata clusterings. This cell wall matrix differentiation persists in cell contacts of mature MCs. Simultaneously, the wall bands between those of future cell contacts differentiate with (1) deposition of local cell wall thickenings including cellulose microfibrils, (2) preferential presence of MLGs, (3) absence of callose and (4) transient presence of the pectins identified by the JIM5 and JIM7 antibodies. The wall areas between cell contacts expand determinately to form the cell isthmi and the cell lobes.
• *Conclusions* The morphogenesis of lobed MCs is characterized by the early patterned differentiation of two distinct cell wall subdomains, defining the sites of the future MC contacts and of the future MC isthmi respectively. This patterned cell wall differentiation precedes cortical microtubule reorganization and may define microtubule ring disposition.

Key words: Callose, cell contacts, microtubules, mixed-linkage glucans, lobed cell morphogenesis, pectin epitopes, *Zea mays*.

INTRODUCTION

Morphogenesis of the lobed mesophyll cells (MCs) is an important phenomenon because it is highly controlled and results in intercellular space formation (Panteris and Galatis, 2005). The labyrinth of intercellular spaces in mesophyll is crucial for leaf function, since it enables photosynthesis, transpiration and respiration (Mauseth, 1988, 1998). In MC morphogenesis, the cortical microtubules play a key role. At the onset of MC shaping, they are re-arrayed into cortical microtubule rings arranged transverse to the longitudinal cell axis. Their assembly is followed by deposition of cellulose microfibril rings in the adjacent cell wall regions, which become locally thickened. This differentiation enables definite regions of the longitudinal cell walls to follow a strictly controlled pattern of growth. The cell wall areas reinforced by the cellulose microfibril rings are unable to grow in diameter, thus becoming cell isthmi, while the intervening cell wall areas expand significantly and form cell lobes. As a result, the cell wall areas reinforced by the cellulose microfibril rings start to detach from each other, initiating schizogenous intercellular spaces (Jung and Wernicke, 1990, 1991; Apostolakos *et al.*, 1991; Wernicke and Jung, 1992; Panteris *et al.*, 1993*a*; Panteris and Galatis, 2005). The mechanism described above functions during morphogenesis in different types of lobed cells, even in the most asymmetrical ones (Galatis, 1988; Wernicke *et al.*, 1993; Panteris *et al.*, 1993*a*, *b*; Panteris and Galatis, 2005).

This work attempts to examine in MCs of the poaceous *Zea mays* (1) whether the pattern of microtubule reorganization is preceded by another pattern that could define or affect the pattern of microtubule ring disposition, and (2) the mechanism that defines the cell wall regions that will become MC contacts. At the sites of MC contacts of *Zea mays*, the plasmodesmata occur in clusters. They are of primary importance for MC function because they mediate the transfer of photosynthetic assimilates towards the sheath of the vascular bundles (Evert *et al.*, 1977).

The local differentiation of cell wall matrix polysaccharides is related to (1) the establishment and maintenance of the cell contacts and (2) the cell wall detachment (Knox, 1992; Jarvis *et al.*, 2003; Ordaz-Ortiz *et al.*, 2009; Lee *et al.*, 2011). Among other pectins, de-esterified homogalacturonans (HGAs) linked through xyloglucans contribute to the maintenance of cell adhesion (Willats *et al.*, 2001; Ordaz-Ortiz *et al.*, 2009), while the partially methyl-esterified HGAs and some hemicellulose epitopes

seem to facilitate cell wall detachment (Orfila *et al.*, 2001; Willats *et al.*, 2001, 2004; Ordaz-Ortiz *et al.*, 2009).

In accordance with the above, the following phenomena were investigated in differentiating MCs of *Zea mays*: (1) plasmodesmata distribution along cell walls, particularly the longitudinal ones, and (2) the chemical differentiation of the MC cell wall matrix, especially in the cell wall areas resisting splitting during intercellular space formation, where cell contacts will form. The latter phenomenon was approached by examination of the distribution in MC walls of the hemicelluloses callose and (1 → 3,1 → 4)-β-D-glucans (MLGs) and of the pectins carrying the epitopes detected by 2F4, JIM5, JIM7 and LM6 antibodies, at different stages of MC development.

MATERIALS AND METHODS

Plant material

This study was carried out in leaves of *Zea mays* 'Aris'. Seedlings were grown in small beakers on filter paper soaked with distilled water for 3–7 days in darkness at 25 ± 1 °C or in room conditions for 20 d. *Zea mays* caryopses were kindly provided by the National Agricultural Research Foundation, Cereal Institute, Thessaloniki, Greece.

Microtubule immunolocalization

Zea mays paradermal leaf sections were initially fixed in paraformaldehyde (8 % w/v) in PME buffer (50 mM 1,4-piperazinediethanesulfonic acid, 5 mM $MgSO_4$, 5 mM ethylene glycol tetraacetic acid, pH 6·8) for 45 min at room temperature. After thorough washing with PME, the material underwent mild cell wall digestion with 1 % (w/v) cellulase (Onozuka Yakult, Honsha, Tokyo, Japan), 1 % (w/v) Macerozyme R-10 (Onozuka Yakult, Honsha, Tokyo, Japan), 1 % (v/v) glucuronidase (Sigma) and 2 % (w/v) driselase (Sigma) in PME, pH 5·6, for 15 min. Following rinsing with PME, the material was treated for 20 min with 0·5 % (v/v) Triton X-100 and 2 % (v/v) dimethyl sulfoxide (DMSO) in phosphate-buffered saline (PBS), pH 7·4. The samples were washed with PBS containing 1 % (w/v) bovine serum albumin (BSA), followed by overnight incubation at room temperature with rat monoclonal anti-α-tubulin antibody clone YOL 1/34 (Serotec, Oxford, UK) diluted 1 : 40 in PBS containing 1 % (w/v) BSA. After rinsing with PBS containing 1 % (w/v) BSA, the samples were incubated with fluorescein isothiocyanate (FITC)-conjugated anti-rat immunoglobulin G (IgG) (Sigma) diluted 1 : 40 in PBS containing 1 % (w/v) BSA, for 2 h at 37 °C. Following washing with PBS, the DNA was stained for 5 min with 10 μg ml^{-1} Hoechst 33258 (Sigma) in PBS and the samples were mounted with an anti-fade solution [2·4 mg *p*-phenylenediamine (Sigma) diluted in 1·5 ml of a solution containing 2 : 1 glycerol : PBS].

Endoplasmic reticulum immunolocalization

For endoplasmic reticulum (ER) immunostaining, the microtubule labelling protocol was applied with the addition of the following antibodies: 2E7 [(Santa Cruz Biotechnology; HDEL (2E7): sc-53472)] as first antibody and FITC-conjugated anti-mouse IgG (Sigma) as second antibody (for details see Giannoutsou *et al.*, 2011).

Callose localization

Callose in living *Z. mays* mesophyll was localized in hand-made leaf sections stained with 0·05 % (w/v) aniline blue (Sigma, C.I. 42725) in 0·07 M K_2HPO_4 buffer, pH 8·5 (O'Brien and McCully, 1981).

For callose immunolocalization in semi-thin sections, small pieces of leaf were fixed in 2 % (w/v) paraformaldehyde and 0·1 % (v/v) glutaraldehyde in PME at 4 °C for 1·5 h. The specimens were washed in the same buffer and dehydrated in a graded ethanol series (10–90 %) diluted in distilled water and three times in absolute ethanol, each step lasting 30 min, at 0 °C. The material was post-fixed with 0·25 % (w/v) osmium tetroxide added to the 30 % ethanol step for 2 h. The material was infiltrated with LR White (LRW) (Sigma) acrylic resin diluted in ethanol in 10 % steps to 100 % (1 h in each) at 4 °C and with pure resin overnight. The samples were embedded in gelatin capsules filled with LRW resin and polymerized at 60 °C for 48 h.

Semi-thin sections of material embedded in LRW resin were transferred to glass slides and blocked with 5 % (w/v) BSA in PBS for 5 h. After washing with PBS, anti-(1 → 3)-β-D-glucan antibody (Biosupplies Australia, Parkville, Australia) diluted 1 : 40 in PBS containing 2 % (w/v) BSA was applied overnight at room temperature. Following rinsing with PBS and blocking again with 2 % (w/v) BSA in PBS, the sections were incubated for 1 h at 37 °C in FITC anti-mouse IgG (Sigma) diluted 1 : 40 in PBS containing 2 % (w/v) BSA. After rinsing with PBS, the sections were mounted using an anti-fade medium containing *p*-phenylenediamine.

Callose immunolocalization was also carried out in hand-made leaf sections. The sections were fixed in 8 % (w/v) paraformaldehyde in PME for 45 min at room temperature, washed three times for 15 min with PME and treated with 1 % (w/v) cellulase in PME, pH 5·6, for 60 min. After washing with PME, the sections were extracted with 0·5 % (v/v) Triton X-100 and 2 % (v/v) DMSO in PBS for 20 min and transferred to PBS containing 2 % (w/v) BSA for 1 h. The sections were incubated with anti-callose antibody overnight and rinsed with PBS three times, each for 15 min. They were transferred to PBS containing 2 % (w/v) BSA and incubated in FITC IgG as described above, washed with PBS and covered with anti-fade solution.

Callose immunogold localization was carried out in thin sections of material embedded in LRW resin mounted on gold grids. They were treated with PBS for 30 min, blocked with 5 % (w/v) BSA in PBS for 3–5 h, incubated with anti-callose antibody for 2·5 h at 37 °C and finally incubated with 10 nm monodisperse colloidal gold-conjugated anti-mouse IgG (Sigma) overnight. Anti-(1 → 3)-β-D-glucan antibody and gold-conjugated IgG were diluted 1 : 40 and 1 : 10 in blocking buffer respectively. The sections were counterstained with 2 % (w/v) aqueous uranyl acetate for 20 min.

MLG localization

For immunolocalization of these mixed-linkage glucans, an antibody recognizing linear (1 → 3,1 → 4)-β-oligosaccharide segments (Biosupplies Australia) was used, following the protocol described for callose immunolocalization.

Homogalacturonan localization

HGAs are composed of 1,4-linked α-D-galactosyluronic acid (GalA) residues (Fry, 2011). Some of their carboxyl groups are

methyl-esterified. HGAs with a low degree of methyl esterification readily form ordered structures (gels) in the presence of calcium ions (Fry, 1990; Michelli, 2001). JIM5 and JIM7 monoclonal antibodies recognize different patterns of methyl esterification on HGAs; the JIM5-HGA epitope contains few or no methyl esters, whereas the JIM7-HGA epitope is more heavily methyl-esterified (Knox *et al.*, 1990). The 2F4 monoclonal antibody recognizes non-esterified HGAs that are cross-linked by calcium (Liners *et al.*, 1989; Douchiche *et al.*, 2010; Eder and Lütz-Meindl, 2010).

For immunolabelling of the above HGA epitopes in fixed freehand and semi-thin leaf sections, the labelling protocol described above for callose localization was used by adding JIM5, JIM7 and 2F4 (PlantProbes, Leeds, UK) as primary antibodies and FITC-conjugated anti-rat IgG (Sigma) as second antibody in all cases. All antibodies were diluted in PBS that contained 2 % (w/v) BSA, except for 2F4 and its second antibody, which were diluted in T/Ca/S buffer (Tris–HCl 20 mM, pH 8·2, $CaCl_2$ 0·5 mM, NaCl 150 mM).

Rhamnogalacturonan localization

The rhamnogalacturonans (RGAs) are a family of closely related polysaccharides containing branched and linear α-L-Ara*f* and β-D-Gal*p* residues (Ridley *et al.*, 2001; Fry, 2011). LM6 antibody (Plant Probes) recognizes 1,5-linked α-arabinans and can bind more readily to highly branched arabinans (Willats *et al.*, 1998).

Immunolabelling of the LM6-RGA epitope was performed on fixed freehand and semi-thin leaf sections, using the labelling protocol previously described for callose localization, adding LM6 as primary antibody and FITC-conjugated anti-rat IgG (Sigma) as second antibody (Douchiche *et al.*, 2010; Eder and Lütz-Meindl, 2010).

Transmission electron microscopy and light microscopy

Small pieces of *Z. mays* leaves were fixed in glutaraldehyde, post-fixed in osmium tetroxide, dehydrated in an acetone series and embedded in either Durcupan ACM (Fluka) or Spurr's mixture (Serva, Heidelberg, Germany). Thin sections were stained with uranyl acetate and lead citrate. Semi-thin sections were stained with 0·5 % (w/v) toluidine blue in 1 % (w/v) borax solution.

Observation and photography

Semi-thin and hand-made sections were examined with a Zeiss Axioplan microscope equipped with a UV source, a differential interference contrast (DIC) optical system, the proper filters and a Zeiss Axiocam MRc5 digital camera. Aniline blue-stained sections were examined using a filter set provided with a 365 nm exciter solid glass filter and a 420 nm barrier longwave pass band filter, and immunolabelled sections were examined with a filter set provided with a 450–490 nm exciter pass band filter and a 515–565 nm barrier pass band filter. All samples were checked for UV autofluorescence using the above filters. Both transmission electron microscopy (TEM) and immuno-TEM specimens were examined with a Philips 300 transmission electron microscope.

RESULTS

General remarks

In sections vertical to the long leaf axis (transverse sections), most of the photosynthetic MCs of *Z. mays* are radially arranged around the sheath of vascular bundles (Evert *et al.*, 1977; see also Supplementary Data Fig. S1). Depending on their position in the mesophyll, they exhibit significant differences in shape, size and number of lobes. A single layer of MCs, appearing as palisade-like in transverse leaf sections, is intercalated between epidermis and bundle sheath cells on both leaf surfaces (Metcalfe, 1960; see also Supplementary Data Fig. S1). In sections parallel to the leaf surface (paradermal sections), they appeared very elongated, were arranged with their longer axis parallel to the leaf axis and usually displayed up to six lobes (Fig. 1A). MC isthmi, vertical to the leaf axis, formed at the cell walls that were parallel to the leaf axis (longitudinal cell walls) (Fig. 1A). The MCs lateral to the vascular bundles were shorter and wider than the palisade-like MCs. They showed deep isthmi and often exhibited cell branches contacting one or more bundle sheath cells along relatively large cell wall areas (Fig. 1B). In leaf areas where the vascular bundles laid close to one another, one layer of MCs intervened between bundle sheaths (Fig. 1C). These MCs formed one or two isthmi transverse to the vascular bundle axis and exceptionally one isthmus parallel to it (Fig. 1C).

MC initials

The MCs are generated in an acropetal fashion by a meristematic zone localized at the base of the leaf (Mauseth, 1988). Considering the differences in shape and size characterizing the MCs, it seems likely that different MC initials give rise to different MC types. Before differentiation commenced, the MC initials underwent some division(s), during which cell walls aligned transversely to the long leaf axis (transverse cell walls) were laid down (Fig. 2A). Then, MC initials grew in size parallel to the leaf axis, a process resulting in substantial elongation of the longitudinal cell walls (Fig. 2B; cf. Fig. 2A). These walls appeared relatively thin and are interrupted by few, usually single, plasmodesmata (Fig. 2I). In addition, the longitudinal MC walls were lined by symmetrically distributed cortical microtubules (Fig. 2J_1). At this stage, intercellular spaces were generated at the sites of junction of three or more MC initials (Fig. 2B inset, C), which became intercellular canals along MC edges (see also Panteris *et al.*, 1993*a*).

After aniline blue staining and callose immunolabelling, fluorescent callose spots were found along the whole surface of the longitudinal and transverse MC walls (Figs 2C and 3A_1, A_2). Callose was also deposited in the walls delimiting the intercellular spaces at the junctions of the MC initials (Fig. 2C).

MLGs were found along the whole surface of the longitudinal and transverse walls of the MC initials (Figs 2D and 3A_1, A_2). The 2F4-HGA epitope was also localized along the whole surface of the walls of these cells (Fig. 3A_3, A_4). The longitudinal walls labelled with this antibody emitted a poor fluorescence signal, while the transverse ones emitted a more intense signal (Fig. 2E). The walls outlining the intercellular canals also fluoresced.

The JIM5-HGA epitope was mainly localized in the cell wall regions delimiting the intercellular spaces generated at the

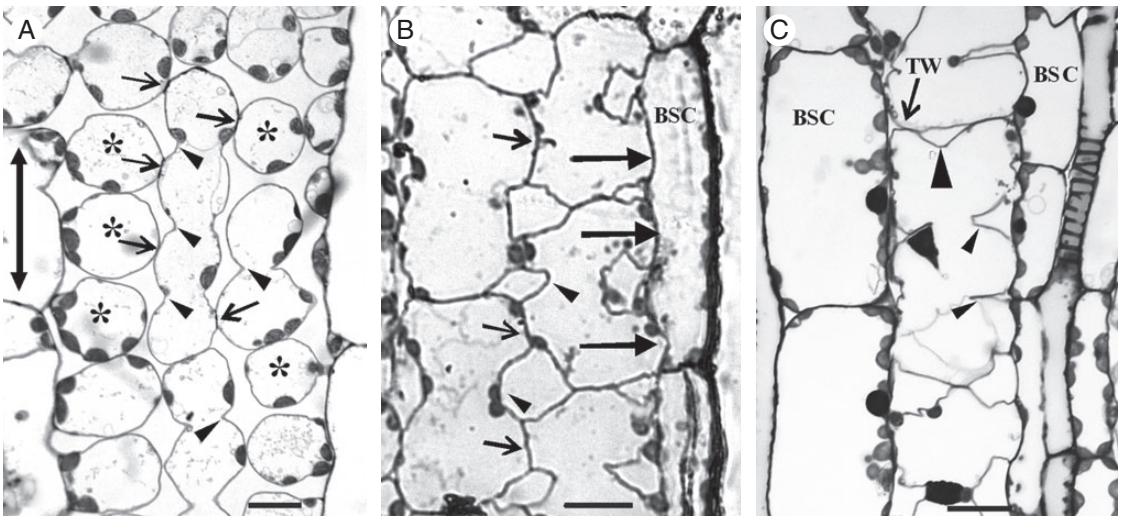

FIG. 1. Paradermal sections of MCs as they appear in the light microscope after staining with toluidine blue. (A) Palisade-like MCs in paradermal view. Arrows indicate cell contacts and arrowheads cell isthmi. Asterisks mark cell lobes in an external paradermal semi-thin section. The double arrow indicates the leaf axis in (A–C). (B) MCs were located laterally to vascular bundles. Large arrows show contacts of MCs with bundle sheath cells. Small arrows point to MC contacts and arrowheads to MC isthmi. BSC, bundle sheath cell. (C) A single layer of MCs intervenes between two adjacent vascular bundles. The large arrowhead indicates a cell isthmus parallel to the leaf axis, while the small arrowheads show cell isthmi transverse to the leaf axis. TW, transverse wall. Scale bars = 10 μm.

junctions of the MC initials (Figs 2F and 3A_5, A_6). Intense fluorescence signal was also emitted by the areas where the transverse walls met the longitudinal walls (Figs 2F and 3A_6). The JIM7-HGA epitope had limited participation in the cell wall matrix of the MC initials. In contrast, the junctions of cell walls delimiting the intercellular spaces among the MC initials emitted an intense fluorescent signal (Fig. 2G). In the triangular intercellular space illustrated in the inset in Fig. 2G, the signal was emitted by two of the cell wall junctions but not by the third, where the cell wall detachment continued. The LM6-RGA epitope marked the walls delimiting the intercellular spaces formed at the MC junctions only (Fig. 2H).

Nascent and young MCs

The first structural signs of MC differentiation were manifested in the cell walls of nascent MCs. Aniline blue staining and callose immunolabelling revealed that callose disappeared from most cell walls regions (Fig. 4A, B; cf. Fig. 2C). However, this polysaccharide was found in definite regions of the longitudinal cell walls, forming two to five callose patches in each wall, 2–3 μm in width (Figs 3B_1, B_2 and 4A, B). The cell walls of nascent and differentiating MCs that were not stained with aniline blue or immunolabelled for callose did not emit any fluorescence when they were observed with an epifluorescence microscope under the filters used for callose localization after aniline blue staining, as well as after immunodetection (Supplementary Data Fig. S2). Therefore, the callose patches do not represent cell wall autofluorescence, but real callose depositions.

The callose patches were arranged at regular distances from each other and were usually localized in the same planes on the two opposite longitudinal MC cell walls (Figs 3B_1, B_2 and 4B, E). In young MCs, the distance between two successive callose patches varied from $4{\cdot}16 \pm 0{\cdot}24$ to $4{\cdot}68 \pm 0{\cdot}07$ μm (Table 1). The periclinal longitudinal MC walls showed accumulations of distinct callose spots on the same planes as those of the anticlinal longitudinal ones displaying callose patches (Fig. 4C, D; see also Supplementary Data Video), a finding confirmed in transverse leaf sections. Thus, in space, the callose patches appeared in parallel cell wall bands 2–3 μm in width, transversely aligned to the longitudinal MC axis (Fig. 4C, D; see also Supplementary Data Video).

The number of cell wall bands impregnated with callose was proportional to MC length (Table 2). In MCs up to 13 μm in length, two cell wall bands impregnated with callose were detected. Those varying in length between 13 and 18 μm exhibited three callose-enriched cell wall bands, while those exceeding 19 μm in length exhibited four callose-enriched cell wall bands. Between neighbouring MCs the callose patches were mostly oppositely arranged (Figs 3B_1, B_2 and 4E; see also Supplementary Data Video), an observation suggesting the co-differentiation of laterally adjacent MCs. In many nascent MCs, callose patches were initially established in one of the longitudinal cell walls (Fig. 4A). The callose patches seemed to appear first in the palisade-like MCs.

Examination of many nascent MCs by TEM revealed a shift in plasmodesmata distribution along the longitudinal cell walls from the dispersed type to the clustered type. At definite regions of these cell walls and close to pre-existing plasmodesmata, secondary plasmodesmata were generated, forming plasmodesmata clusterings (PCs; Fig. 5A, B; see also Fig. 2J_2). The cell wall regions, where PCs were initiated, appeared swollen and displayed electron-transparent materials (Fig. 5A–C). In the adjacent cortical cytoplasm, ER elements as well as dictyosome vesicles were found, while the adjacent plasmalemma regions were convoluted (Fig. 5B, C).

During PC establishment, microtubules were scattered along the whole length of the longitudinal cell walls (Fig. 2J_2). Often, microtubules lined the cell wall regions where PCs developed (Figs 2J_2 and 5C). After immunogold callose labelling, numerous gold grains were deposited on developing PCs (Fig. 5D). The cell wall areas between the PCs displayed very few or no gold

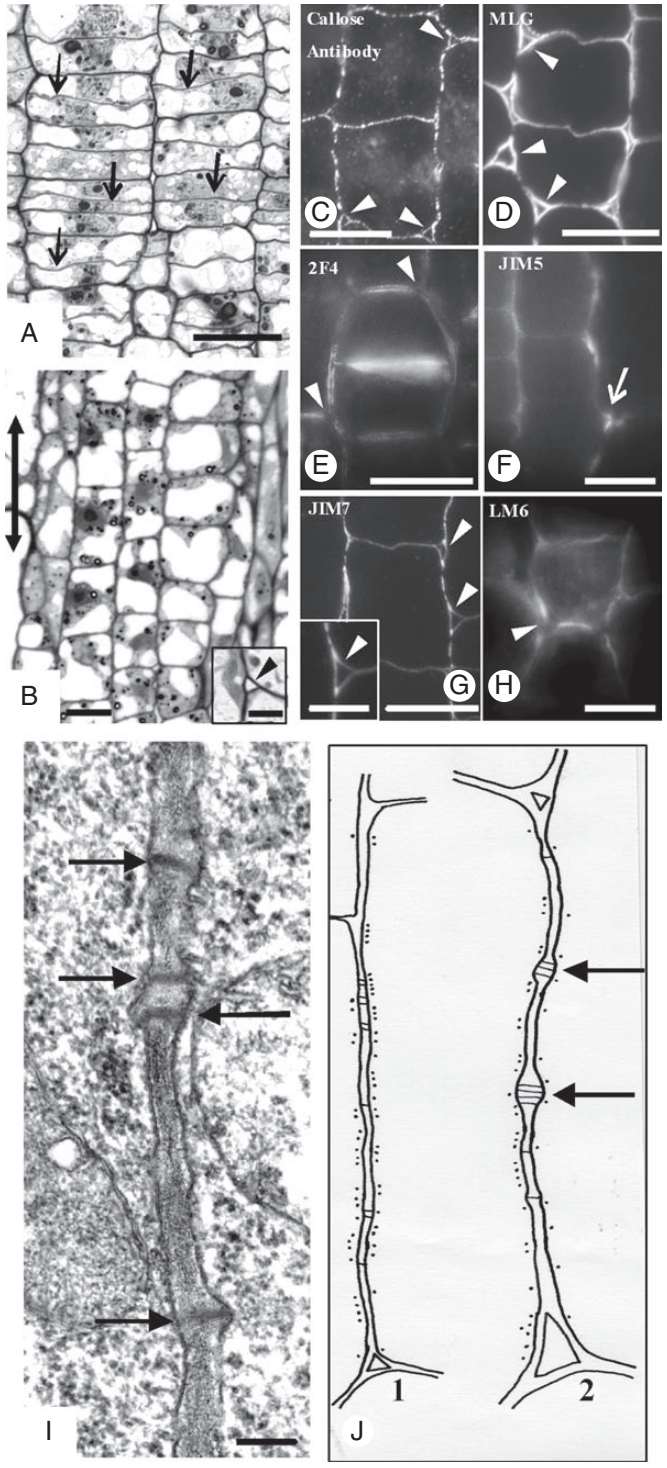

FIG. 2. Micrographs of MC initials taken with a conventional light microscope (A, B), an epifluorescence microscope (C–H) and a TEM (I). (A, B) Paradermal semi-thin sections of MC initials located at the meristematic leaf zone (A) and the region just next to it (B). Arrows in (A) indicate the newly formed transverse cell walls, while the double arrow in (B) indicates the leaf axis in (A–J). (Inset in B) Triangular intercellular space (arrowhead) generated at the junction site of three MC initials. (C–H) Localization of callose (C), MLGs (D) and pectin epitopes (E–H) in cell walls of MC initials. Arrowheads indicate intercellular spaces formed at the junction sites of three or more MC initials. Arrow in (F) shows the junction of a transverse with a longitudinal MC wall. (C, D, G) Immunolabelling in LRW sections. (E, F, H) Immunolabelling in hand-made sections. (I) Longitudinal cell wall portion of an MC initial. Arrows mark plasmodesmata. Scale bars: (A–H) = 10 μm; (I) = 200 nm; (B inset) = 3 μm; (G inset) = 5 μm. (J) Diagram showing the distribution of cortical microtubules along a longitudinal cell wall of a MC initial (J_1) and a nascent MC (J_2). Black dots represent microtubules; black lines represent plasmodesmata. Arrows show young plasmodesmata clusterings.

grains. Thus, the callose patches detected in the epifluorescence microscope demarcate the cell wall regions where PCs develop.

In young MCs the cortical microtubules were reorganized into microtubule rings (Figs 6A and Supplementary Data Fig. S3A, B, D) that control the deposition of local cell wall thickenings, which contained numerous cellulose microfibrils (Supplementary Data Fig. S3B, C). MC isthmi were formed in the region of cell wall thickenings (Supplementary Data Fig. S3A inset). Their formation was accompanied by the formation of schizogenous intercellular spaces, while in the areas between the cell isthmi cell lobes were formed (Supplementary Data Fig. S3A inset, D). In young MCs, the PC callose patches were prominent (Figs 3C_1, C_2 and 6B) and seemed to predict the sites of the future MC contacts. Callose was also deposited in the walls delimiting the intercellular spaces forming at the MC junctions and in those opening at the cell isthmi regions (Figs 3C_1 and 6C, D).

The cortical microtubule rings and the cell wall bands showing PC callose patches alternated along the longitudinal walls (Fig. 6A; cf. Fig. 6B). Each local cell wall thickening lined by microtubule bundles always occurred between two successive PC callose patches (Fig. 6E). The cortical cytoplasm adjacent to the cell walls possessing the PC callose patches was completely devoid of cortical microtubules (Fig. 6E). The repeated TEM observation of (1) nascent MCs displaying developing PCs and microtubules dispersed along the whole of their longitudinal walls (Fig. 2J_2) and (2) young MCs displaying microtubule bundles between successive PCs (Fig. 6E) led to the conclusion that microtubule reorganization follows the establishment of PC callose patches. The measurements presented in Table 2 allow the conclusions that (1) the distance between successive microtubule rings is similar to that between successive callose patches, (2) each microtubule ring forms at the mid-region between two successive callose-enriched cell wall bands, and (3) the number of callose patches and microtubule rings depends on cell length.

Notably, at this stage, the MLGs were removed from the sites of the longitudinal walls, where callose had been deposited (Figs 3C_2 and 7A, B). They were consistently present in the transverse walls (Figs 3C_1, C_2 and 7A), in the thickenings along the longitudinal cell walls (Figs 3C_2 and 7A) and in the cell wall regions delimiting the intercellular spaces forming at the MC isthmus regions and at the MC junctions (Figs 3C_1 and 7A, B). The 2F4-HGA epitope was gradually removed from the major part of the cell wall surface and was restricted to the sites of the future MC contacts, where callose had been deposited, and to cell wall regions limiting the intercellular spaces at MC junctions (Figs 3C_3, C_4 and 7C). The JIM5-HGA epitope marked only the junctions of the walls delimiting the intercellular spaces at MC junctions and those at the cell isthmus regions (Figs 3C_5, C_6 and 7D–F). The JIM7-HGA epitope enriched the developing local cell wall thickenings (Figs 3C_6 and 7G) and the cell wall regions defining the developing intercellular spaces (Figs 3C_5 and 7G). The LM6-RGA epitope was restricted to the margins of the future cell contacts (Figs 3C_3, C_4 and 7H).

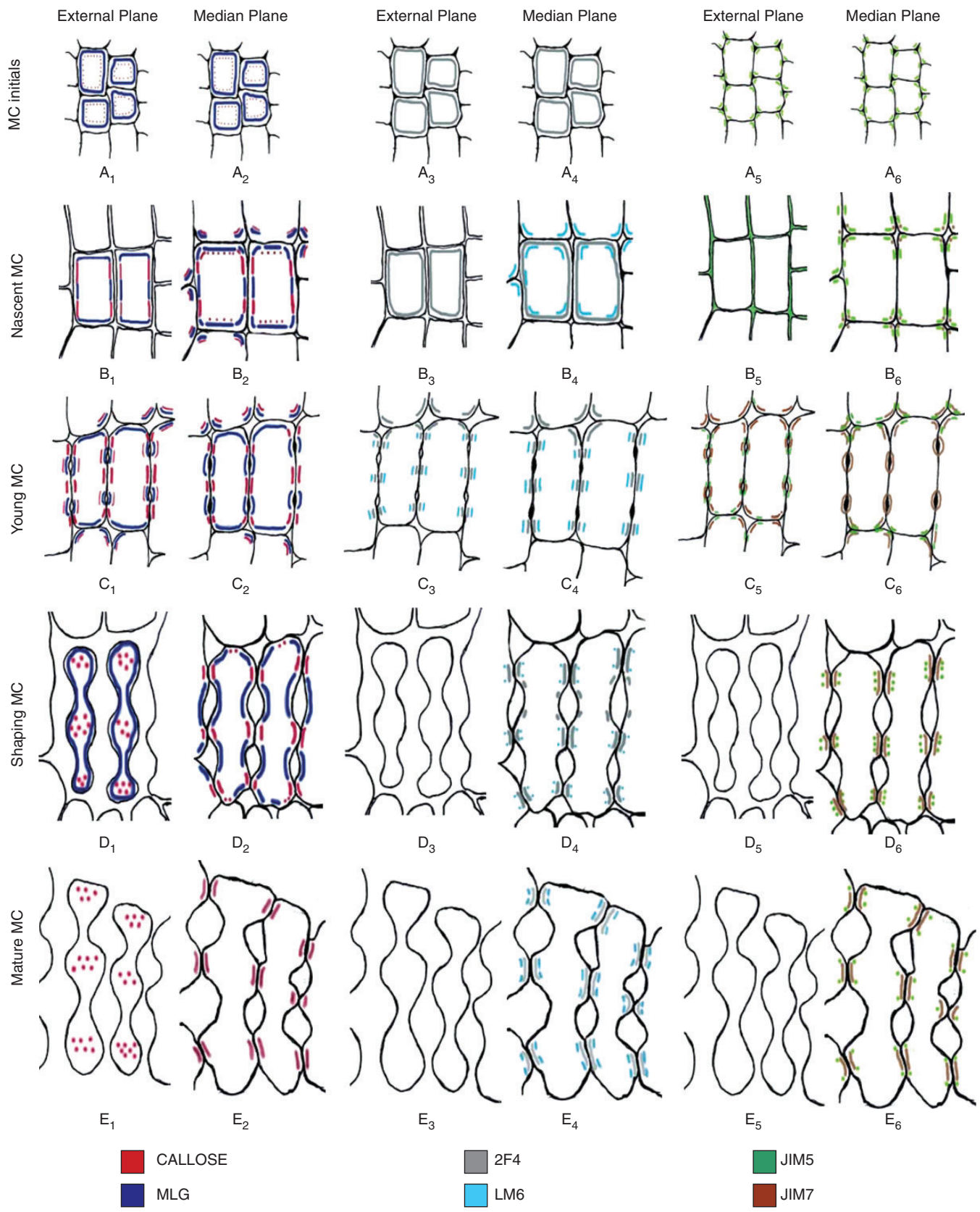

FIG. 3. Diagrams illustrating the distribution of the hemicelluloses callose and MLGs (first two columns) and pectin epitopes (remaining columns) in MC walls at successive stages of MC differentiation. Cells in (A–C) are shown at higher magnification than those in (D, E).

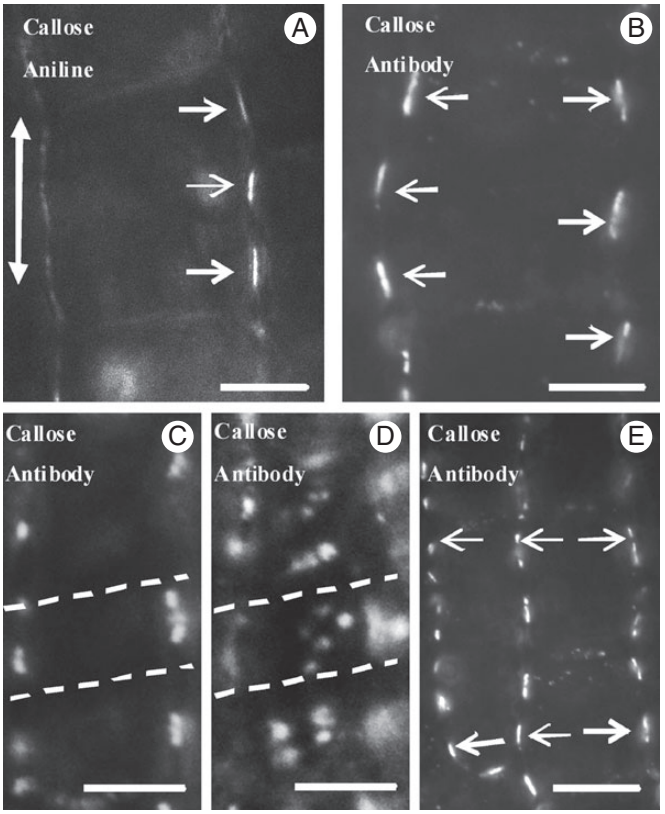

FIG. 4. Callose detection in hand-made sections of nascent MCs. (A, B) Nascent MCs after aniline blue staining (A) and callose immunodetection (B). In longitudinal cell walls, well-defined callose patches (arrows) have been deposited in the cell wall regions where the cell contacts will be formed. The double arrow defines the leaf axis in (A–E). (C, D) Nascent MCs after callose immunodetection in optical sections through a median (C) and an external (D) plane. Dotted lines define a cell wall band impregnated with callose. (E) Callose patches (arrows) in adjacent nascent MCs display an opposite arrangement. Scale bars: (A, B) = 5 μm; (C–E) = 10 μm.

In the latter, both callose and the 2F4-HGA epitope were consistently found (Fig. $3C_1$–C_4).

Shaping MCs

The increase in MC diameter at forming MC lobes, as well as MC elongation, was obvious in shaping MCs. This differential MC growth seemed to create mechanical tensions that forced further cell wall detachment, making the cell isthmi and cell lobes more evident (lower inset in Fig. 8A; see also Apostolakos *et al.*, 1991; Panteris and Galatis, 2005). The cell wall expansion occurring in developing MC lobes did not affect PC integrity (Fig. 8A, C). Actually, MC wall detachment stopped at the PC regions (Fig. 8A, B) that finally resided at the tips of MC lobes, where the MCs contacted each other (Fig. 8C). In shaping MCs, the PCs occupied a greater part of the longitudinal walls and displayed more plasmodesmata than those in young MCs (Fig. 8A, C). The presence of ER in the close vicinity of PCs was obvious in thin MC sections (Fig. 8A) as well as in MCs immunolabelled for HDEL ER proteins (upper inset in Fig. 8A).

In shaping MCs, intense callose depositions were found at the MC contacts (Figs $3D_2$ and 9A) and at the junctions of the cell walls delimiting the intercellular spaces initiated at the MC isthmi, where wall detachment continued. The fluorescent signal emitted by the MC contacts was either continuous or restricted to two or more areas (Fig. 9A). The MC contacts usually displayed more than one PC (Fig. 8C). In shaping MCs, MLGs were found along the whole wall, except for the MC contacts (Figs $3D_1$, D_2 and 9B). A more intense fluorescent signal was emitted by the walls outlining the forming intercellular spaces at the MC isthmus regions (Fig. 9B). Following immunolabelling with 2F4 antibody, an intense fluorescence signal was emitted by the MC contacts (Figs $3D_4$ and 9C) and a very weak signal was emitted by the detaching regions of walls delimiting the intercellular spaces initiated at MC isthmi (Fig. $3D_4$). The JIM5-HGA epitope marked the MC contacts only (Figs $3D_6$ and 9D). These sites emitted a dotted pattern of fluorescence. The JIM7-HGA epitope was also restricted to cell contacts, but the emitted signal was continuous (Figs $3D_6$ and 9E). The LM6-RGA epitope was limited to the margins of MC contacts (Figs $3D_4$ and 9F).

TABLE 1. *Distance between two successive callose patches in young and mature MCs*

	Longitudinal cell walls with two callose patches	Longitudinal cell walls with three callose patches	Longitudinal cell walls with four callose patches
Young MCs	4·68 ± 0·07 μm	4·40 ± 0·16 μm	4·16 ± 0·24 μm
Mature MCs	10·13 ± 1·45 μm	9·36 ± 0·96 μm	14·12 ± 0·99 μm

TABLE 2. *Distance (μm) between two successive callose patches and two successive microtubule (MT) rings in young MCs*

	Longitudinal cell walls with two callose patches and one MT ring	Longitudinal cell walls with three callose patches and two MT rings	Longitudinal cell walls with four callose patches and three MT rings
Callose patches	4·68 ± 0·07	4·40 ± 0·16	4·16 ± 0·24
Wall length	13·36 ± 0·82	17·52 ± 0·96	19·68 ± 1·35
MT rings	–	4·64 ± 0·23	5·1 ± 0·54
Wall length	12·61 ± 0·76	16·32 ± 0·93	18·57 ± 1·28

Mature MCs

The cell walls of mature MC contacts appeared relatively thick and electron-dense and were traversed by numerous plasmodesmata (Fig. 10 inset). The increased electron density possibly reflects the dominant presence of matrix polysaccharides. In contrast, the cell walls delimiting the MC lobes were relatively electron-transparent (Fig. 10 inset). In each MC contact, the regions traversed by plasmodesmata were slightly thickened (Fig. 10; see also Evert *et al.*, 1977). Each plasmodesma was surrounded by a cylinder of material more electron-transparent than that of the rest of the MC contact (Fig. 10). ER was prominent in the cortical cytoplasm apposed to MC contacts (Fig. 10).

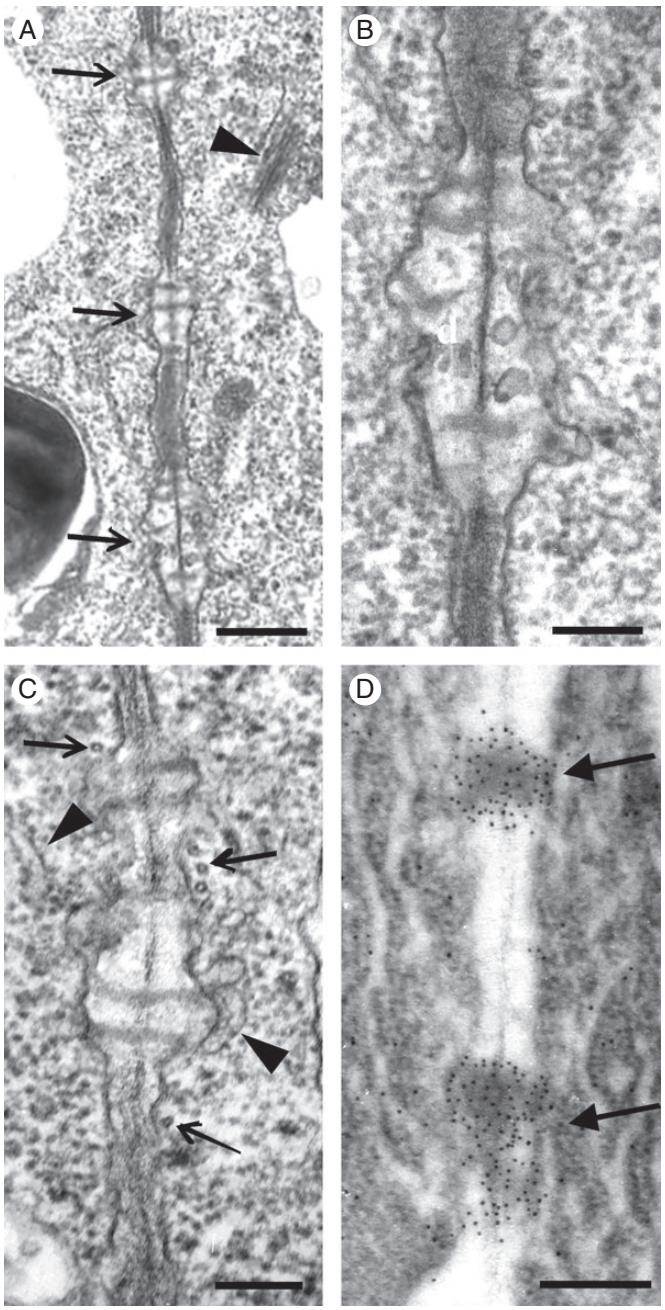

FIG. 5. TEM views of longitudinal cell wall regions of nascent MCs. (A) Cell wall area displaying three young plasmodesmata clusterings (arrows; cf. Fig. 2I). The arrowhead points to a dictyosome. (B, C) Higher magnification of plasmodesmata clusterings. Arrows show microtubules and arrowheads ER portions. (D) Wall area of nascent MC after immunogold callose labelling. Numerous gold grains have been deposited on the forming plasmodesmata clusterings (arrows). Scale bars: (A, D) = 500 nm; (B, C) = 200 nm.

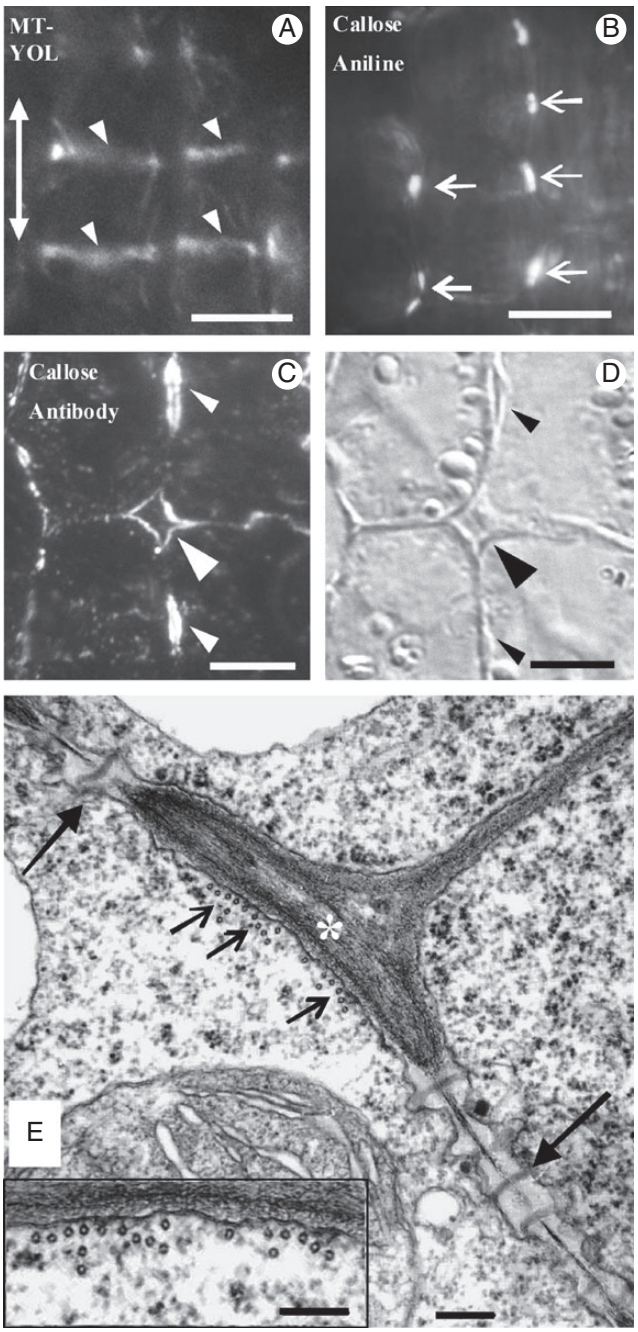

FIG. 6. Epifluorescence microscope (A–C), differential interference contrast (D) and TEM (E) views of young MCs. (A) MC tubulin immunolabelling in hand-made leaf sections. Arrowheads point to microtubule bundles formed in the cortical cytoplasm adjacent to the sites of future cell isthmi. Note that the microtubule bundles between the adjacent MCs have been formed on the same planes. The double arrow indicates the leaf axis in (A–E). (B) Aniline blue staining of MCs in hand-made leaf sections. Arrows mark callose patches at the positions of future cell contacts. (C, D) External paradermal section of young MCs embedded in LRW after callose immunolabelling (C) and with DIC optics (D). Cell walls outlining an intercellular space that has opened between MCs (large arrowhead) and intercellular spaces forming at future cell isthmi (small arrowheads) emit an intense fluorescent callose signal. (E) Microtubule bundle (small arrows) lining a wall thickening (asterisk) deposited in the position of a future cell isthmus. Plasmodesmata clusterings (PCs, large arrows) exist on both sides of the wall thickening. Note the absence of microtubules from the cytoplasm lining the PCs (cf. Fig. 5C). (Inset) Microtubule bundle at higher magnification. Scale bars: (A, B) = 10 μm; (C, D) = 5 μm; (E, E inset) = 200 nm.

In mature MCs, callose was exclusively present in cell contacts (Figs 3E$_1$, E$_2$ and 11A, B). In median optical planes, the fluorescent callose signal was either continuous or dotted (Figs 3E$_2$ and 11A, B), while in external and internal optical planes the signal was emitted by distinct spherical formations (Figs 3E$_1$ and 11C).

The length of the MC contacts was 3·5–4 μm, slightly greater than that of the PC callose patches in young MCs, which was

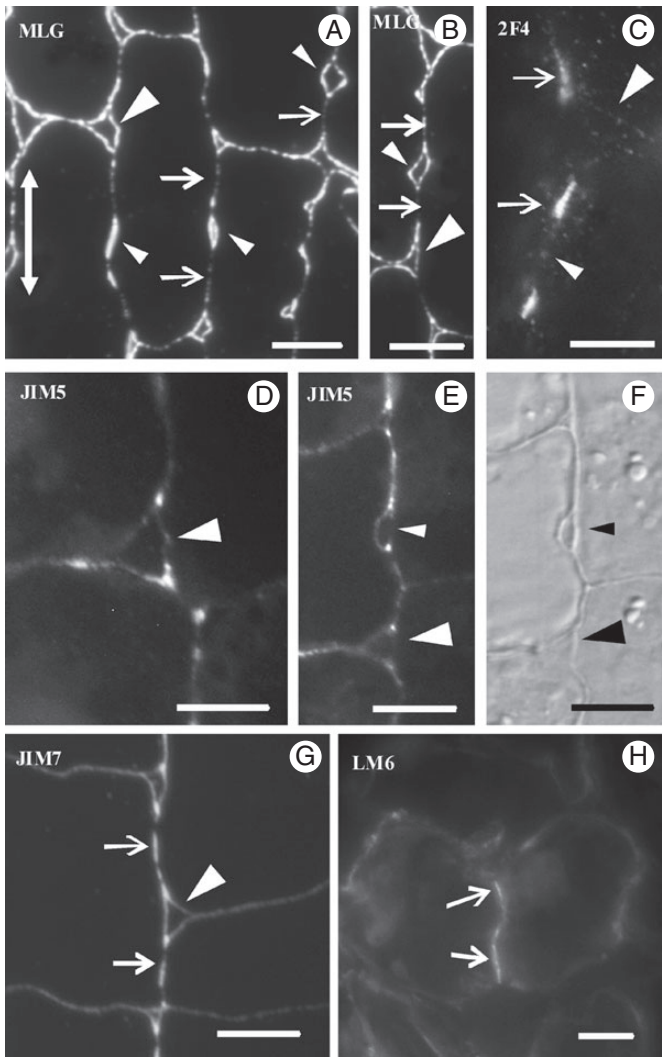

FIG. 7. Immunolocalization of MLGs (A, B) and pectin epitopes (C–H) in young MCs. Arrows mark the positions of future cell contacts, small arrowheads the positions of future cell isthmi and large arrowheads the intercellular spaces at MC junctions. The double arrow in (A) indicates the leaf axis. (A, B, D–G) LRW resin sections; (C, H) hand-made sections. (F) DIC optical view of the cell portion shown in (E). Scale bars = 5 μm.

2–3 μm. While in young MCs the distance between two successive callose patches varied between 4 and 4·5 μm, in mature MCs it varied between 9 and 14 μm (Table 1). Therefore, during MC growth, the cell wall regions intercalated between the callose patches seemed to elongate.

In mature MCs, MLGs were completely absent (Figs 3E$_1$, E$_2$ and 11D), but persisted in vascular bundle cells and in sclerenchymatic fibres (Fig. 11D). The 2F4-HGA and JIM7-HGA epitopes were restricted to MC contacts (Figs 3E$_4$, E$_6$ and 11E, G). The latter epitope exhibited a continuous fluorescent signal along the whole surface of MC contacts (Fig. 11G). In addition, the JIM5-HGA epitope emitted a dotted signal at the margins of the MC contacts only (Figs 3E$_6$ and 11F), which in DIC optics corresponded to detectable local cell wall thickenings (Fig. 11F inset). The median region of the MC contacts emitted a faint signal. In mature MCs, the margins of cell contacts possessed the LM6-RGA epitope (Figs 3E$_4$ and 11H).

DISCUSSION

Establishment and mechanical properties of cell wall subdomains in developing MCs

The present work revealed for the first time that a definite structural and chemical differentiation of cell walls in the young MCs of *Z. mays* establishes two distinct types of cell wall subdomains with different mechanical properties.

The first type includes the wall subdomains defining the sites of contact between the neighbouring MCs, which in mature MCs are restricted to the tips of cell lobes. During MC shaping they do not extend appreciably and during intercellular space formation they prevent cell wall detachment to proceed into cell contacts. Of prime importance for MC differentiation and function is the insertion (in these cell wall subdomains) of secondary plasmodesmata forming distinct PCs (Fig. 8C). The MC contacts also contribute to the mechanical robustness of the developing and mature leaf (see also Knox, 1992; Jarvis *et al.*, 2003).

The second type of cell wall subdomain defines the cell wall regions where the MC isthmi form. They allow elongation and detachment of the adjacent cell wall partners, greatly contributing to MC lobe formation. The measurements presented in Table 1 support the above hypothesis. In young MCs, the two types of cell wall subdomains alternate along the longitudinal MC walls.

The establishment and maintenance of cell contacts are mediated by local differentiation of matrix cell wall polysaccharides (Knox, 1992; Jarvis *et al.*, 2003). In *Z. mays*, the wall subdomains of MC contacts are characterized by (1) deposition of callose and localization of the pectin epitopes recognized by the 2F4, LM6, JIM5 and JIM7 antibodies (Fig. 3), (2) the removal of MLGs (Fig. 3) and (3) the formation of secondary plasmodesmata, which form distinct PCs (Fig. 8A, C). In mature MCs, the PC sites thickened detectably (Fig. 10; see also Evert *et al.*, 1977). The presence of the HGA epitopes in cell contacts has already been described (Willats *et al.*, 2001; Ordaz-Ortiz *et al.*, 2009). However, the presence of large quantities of callose in establishing and mature cell contacts in MCs of *Z. mays*, which was confirmed in those of *Triticum turgidum* (E. Giannoutsou *et al.*, unpubl. res.; see also Supplementary Data Fig. S4), was observed for the first time here.

The wall subdomains among MC contacts showed the following characteristics: (1) the preferential presence of MLGs, which were spread along the whole surface of the extending and splitting cell wall regions, but disappeared before completion of MC morphogenesis (Fig. 3); (2) the temporary presence of the JIM5-, JIM7-HGA and LM6-RGA epitopes (Fig. 3); (3) the deposition of cellulose microfibril rings at the MC isthmus regions (Apostolakos *et al.*, 1991; see also Supplementary Data Fig. S3C); (4) the absence of callose and of the 2F4-HGA epitope (Fig. 3); and (5) the disruption of existing plasmodesmata during wall detachment.

The distribution of the matrix polysaccharides in the MC wall subdomains found in sections of material embedded in LRW after immunolocalization was identical to that observed after immunolocalization in hand-made sections (Fig. 9D, E; cf. Fig. 11F, G). Thus, this distribution is real and not an artefact resulting from the embedding of material in resins (Willats *et al.*, 2001).

It has recently been found that RGA, as well as xyloglucan, xylan and mannan epitopes, can be effectively masked in cell walls by the presence of HGAs (Marcus *et al.*, 2008; Hervé

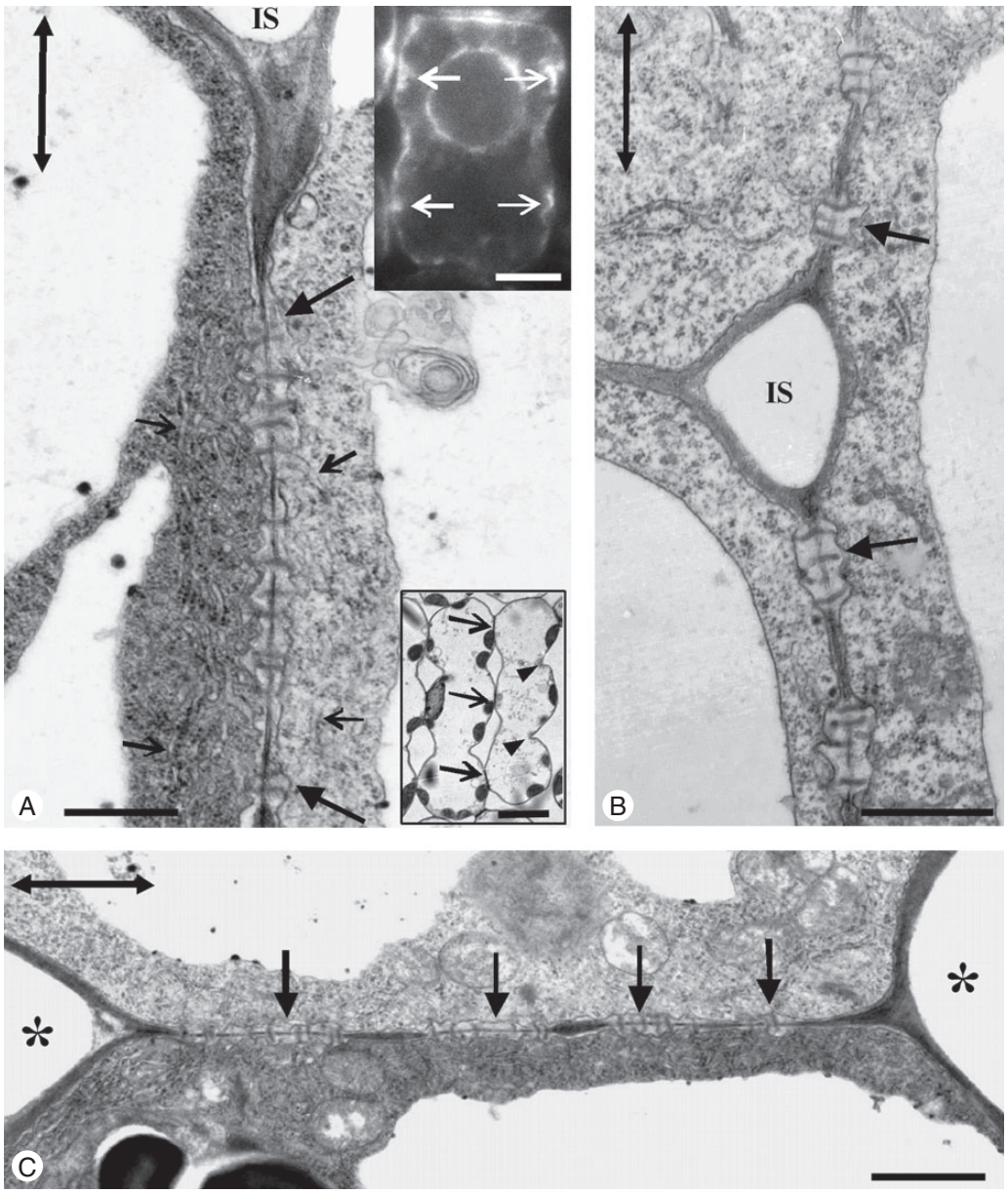

FIG. 8. Shaping MCs as they appear in the light microscope (lower inset in A), in the TEM (A–C) and after ER immunodetection (upper inset in A). (A) Longitudinal view of cell wall portion. Detachment of cell walls forming an intercellular space (IS) at the cell isthmus region stops at the wall region displaying a well-developed plasmodesmata clustering (large arrows). Small arrows point to ER portions, while the double arrow defines the leaf axis. (Upper inset) Immunolabelling of ER HDEL proteins in a shaping MC. The cytoplasm adjacent to the forming cell contacts (arrows) emits an intense fluorescent signal. (Lower inset) Median paradermal semi-thin section of shaping MCs stained with toluidine blue. Arrows show cell contacts and arrowheads show cell isthmi. (B) Triangular intercellular space (IS) formed at the junction of three MCs. Plasmodesmata clusterings (arrows) exist at the regions of the longitudinal wall where cell wall detachment has stopped. The double arrow defines the leaf axis. (C) Forming MC contact. Arrows show plasmodesmata clusterings and asterisks mark intercellular spaces. The double arrow defines the leaf axis. Scale bars: (A) = 500 nm; (A, upper inset) = 5 μm; (A, lower inset) = 10 μm; (B) = 500 nm; (C) = 1 μm.

et al., 2009; Marcus *et al.*, 2010; Wang *et al.*, 2012). Thus, these polysaccharides were detected in cell walls by immunolabelling methods only when the HGAs had been previously removed. Therefore, the question of whether the distribution pattern of callose, MLGs and LM6-RGA epitope in developing MCs (Fig. 3) is affected by masking from HGA epitopes arises. However, our data revealed that in the same cell wall areas of developing MCs, callose as well as MLGs were localized together with 2F4-, JIM5- and JIM7-HGA epitopes (Fig. 3). Therefore, the specific pectin [2F4, JIM5 and JIM7] HGA epitopes do not mask callose and MLGs. In addition, the fact that, in developing MCs, the LM6-RGA epitope is co-localized with the HGA epitopes studied (Fig. 3) shows that the LM6-RGA epitope is not effectively masked by HGAs (Marcus *et al.*, 2008). For further documentation of the above, immunolocalization of callose and MLGs in semi-thin sectioned MCs embedded in LRW has been performed. Pectins were previously removed from these MC cell walls by treatment of sections with 1 M

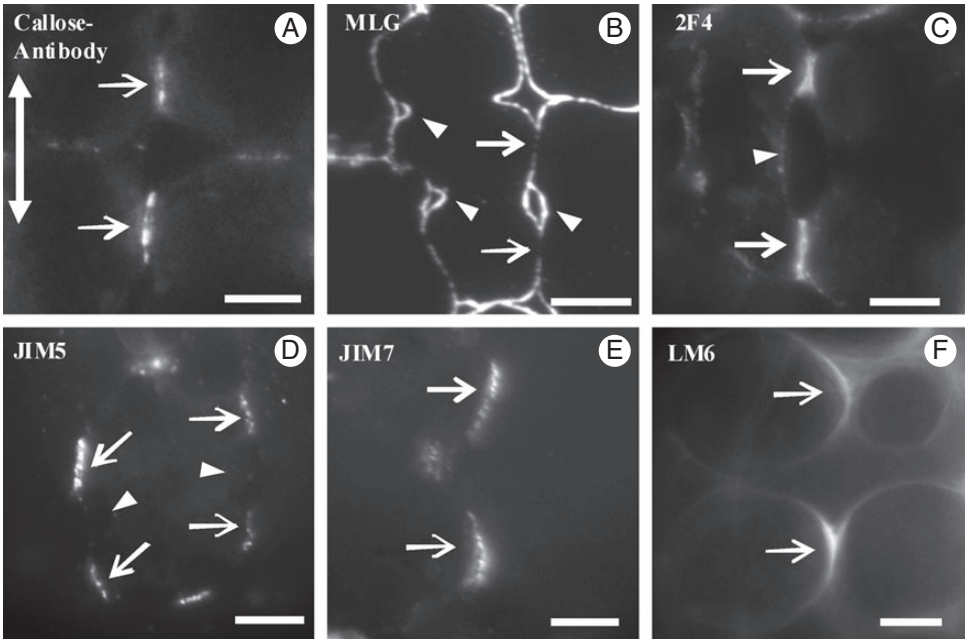

FIG. 9. Immunolocalization of callose (A), MLGs (B) and pectin epitopes (C–F) in shaping MCs. Arrows point to MC contacts, the double arrow defines the leaf axis and arrowheads point to positions of MC isthmi. Scale bars = 5 μm.

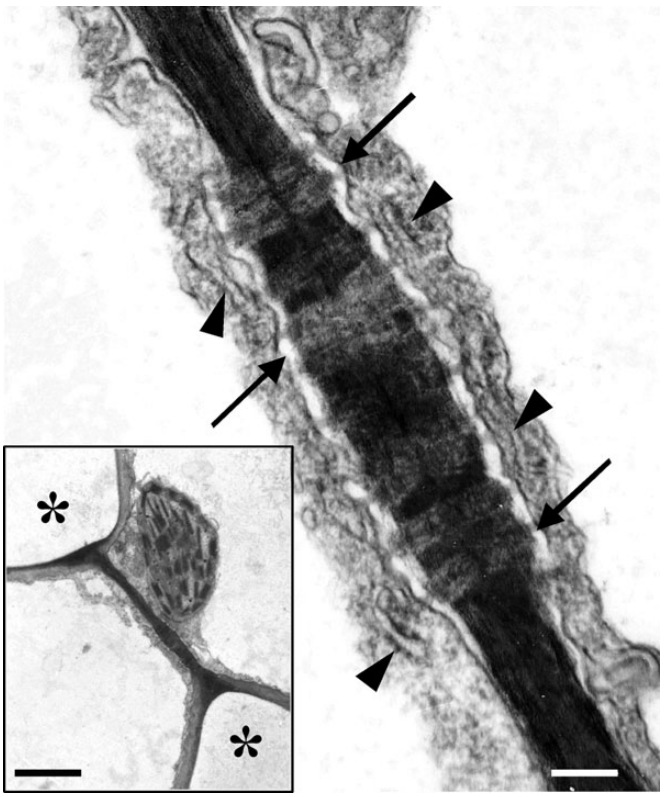

FIG. 10. TEM micrograph of a mature MC contact traversed by plasmodesmata (arrows). Arrowheads point to ER elements. Scale bar = 200 nm. (Inset) The MC contact of which part is shown in Fig. 10 at higher magnification. Asterisks mark intercellular spaces. Scale bar = 2 μm.

KOH for 1 h at 25 °C (Marcus *et al.*, 2010; Wang *et al.*, 2012). In Supplementary Data Fig. S5A_1–D_2 it is obvious that pretreatment with KOH removed HGA epitopes from MC cell walls (Supplementary Data Fig. S5A_1, C_1; cf. Fig. S5B_1, D_1). However, in MCs pretreated with KOH, the distribution patterns of callose and MLGs were identical to those of control MCs (Supplementary Data Fig. S5F, H; cf. Fig. S5E, G). Therefore, masking phenomena do not seem to have affected the data obtained in the present work.

Probable roles of matrix polysaccharides in cell wall subdomains

Callose. Callose is a unique (1 → 3)-β-D-glucan that can be formed and removed from the cell wall in a short time, and is involved in a variety of developmental processes, including its deposition in cell wall regions experiencing mechanical stress (Heslop-Harrison, 1964; Stone and Clark, 1992; Basic *et al.*, 2009; Chen and Kim, 2009; Galatis and Apostolakos, 2010; Piršelová and Matušiková, 2012). Only hypotheses can be made about the function(s) of callose in the wall subdomains of MC contacts. Thus, callose, apart from its well documented involvement in the control of plasmodesmata permeability (Xu and Jackson, 2010; Vatén *et al.*, 2011), may serve the following functions.

(1) It may serve as a cell wall-strengthening material (Parre and Geitmann, 2005), possibly making the impregnated cell wall subdomains stiff and not easily extendable. Callose with other matrix polysaccharides deposited in the MC contact wall subdomains may locally prevent the schizogenous separation of the adjacent cell walls. This callose

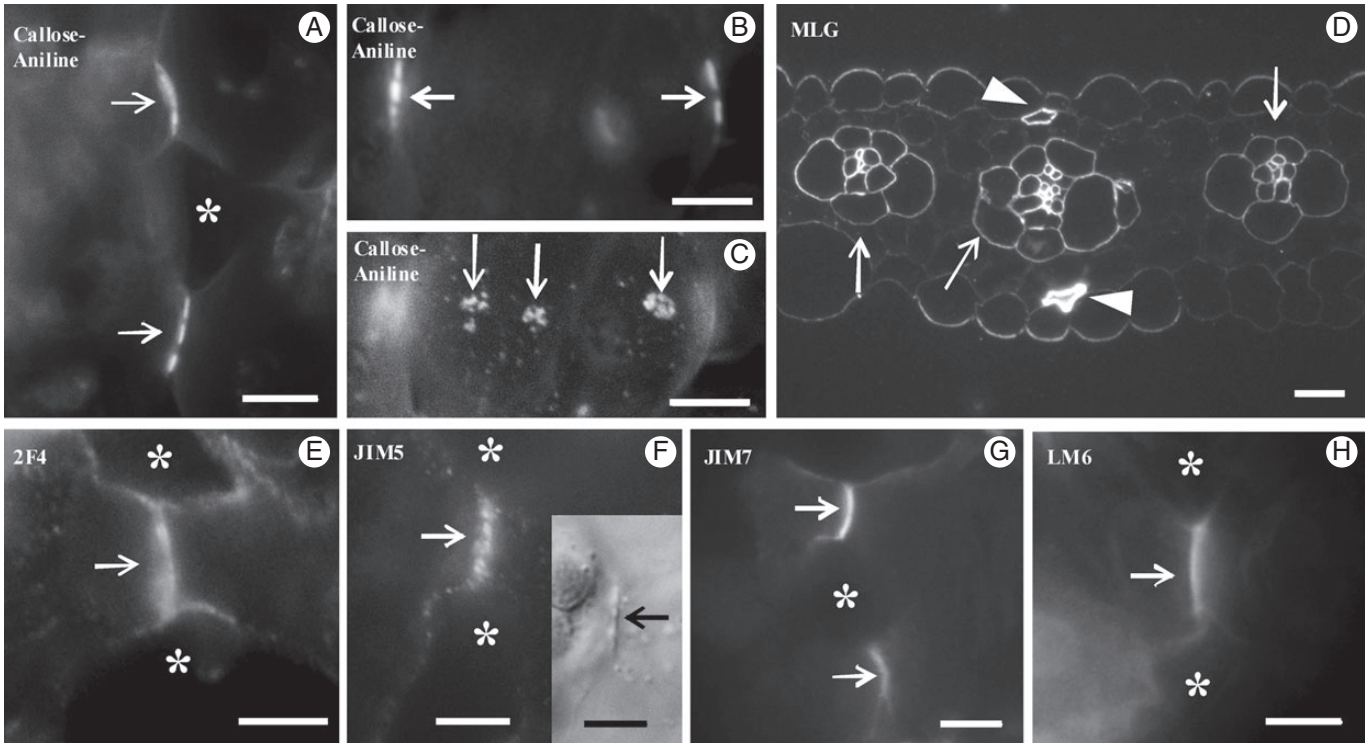

FIG. 11. Localization of matrix cell wall polysaccharides in mature MCs. (A) Localization of callose with aniline blue. The cell wall at the cell contacts (arrows) emits an intense fluorescent signal. Asterisk marks an intercellular space. (B, C) Paradermal optical sections through a median plane (B) and a surface plane (C) of the same MC lobe after aniline blue staining. Arrows show callose depositions at MC contacts of anticlinal (B) and periclinal (C) longitudinal cell walls. (D) Transverse semi-thin section of mature leaf embedded in LRW and immunolabelled for MLGs. MC walls, in contrast to walls of vascular bundle cells (arrows) and sclerenchymatic cells (arrowheads), do not fluoresce. (E–H) Immunodetection of pectin epitopes in hand-made sections of mature MCs. An intense fluorescent signal is emitted by the MC contacts only (arrows). In (H) the section passes through the end of the cell contact. Asterisks mark intercellular spaces. (Inset in F) DIC optical view of MC contact (arrow). Scale bars: (A–C, E–H) = 5 μm; D = 10 μm.

property may protect the plasmodesmata from disruption during MC elongation.

(2) It may participate in secondary plasmodesmata formation. Such involvement has not yet been reported (Ehlers and Kollmann, 2001; Xu and Jackson, 2010). In *Z. mays* MCs, PC development keeps pace with callose deposition, i.e. secondary plasmodesmata form in a callose-enriched wall environment. In this case, callose may (a) facilitate the rapid local digestion of the cell wall, necessary for secondary plasmodesmata formation (Ehlers and Kollmann, 2001) or (b) contribute to the creation of a microenvironment facilitating the duplication of the existing plasmodesmata, a fascinating process recently described for secondary plasmodesmata formation (Faulkner *et al.*, 2008). Notably, callose enriching locally thickened cell wall regions traversed by plasmodesmata has been described in root cells of an *Arabidopsis thaliana* mutant in which genes inducing callose synthesis are over-expressed (Vatén *et al.*, 2011).

The cell walls outlining the developing MC intercellular spaces are temporarily enriched by callose (Fig. 3). This transient callose represents wound callose, which is believed to protect the plasmalemma and the adjacent cell wall regions from the mechanical stresses generated during intercellular space initiation (Parre and Geitmann, 2005; Vaughn *et al.*, 2007; Apostolakos *et al.*, 2009). In contrast, the callose present in mature MC contacts is constitutive callose. The degree of polymerization, age and thickness of the callose deposits may alter the physical properties of this glucan (Stone and Clarke, 1992).

MLGs. These hemicelluloses characterize the cell walls of Poales, to which *Z. mays* belongs (Carpita *et al.*, 2001; Buckeridge *et al.*, 2004; Fincher, 2009*a*) and very rarely cell walls of other vascular plants and lower land plants (Fry *et al.*, 2008; Burton and Fincher, 2009). MLGs that are localized in the cell wall regions between the cell contacts of developing MCs (Fig. 3) may facilitate the preferential and intense cell wall expansion at these areas (Table 1). This is consistent with the current view that in developing organs the MLGs are involved in cell wall expansion (Carpita *et al.*, 2001; Buckeridge *et al.*, 2004; Fincher 2009*a*, *b*). This view is reinforced by the pattern of MLG distribution in developing MCs. The MLGs are first located throughout the surface of expanded walls of MC initials (Fig. 3A_1, A_2). Then, they are removed from contact MC sites that do not expand (Fig. 3B_1–D_2), whereas they persist in the cell wall regions between them (Fig. 3B_1–D_2), which greatly elongate. Finally, they are removed from all cell wall regions when elongation of MCs has been completed (Fig. 3E_1, E_2).

Pectin epitopes. The presence of different pectin epitopes in the cell contacts and in the areas of cell wall detachment has been examined in detail in dicotyledonous plants (VandenBosch *et al.*, 1989; Knox *et al.*, 1990; Orfila *et al.*, 2001; Willats *et al.*, 2001, 2004). Those pectin epitopes that consist of intensely de-esterified HGAs molecules are linked with Ca^{2+} and form cell wall matrix gels of high viscosity, which make wall detachment difficult during intercellular space formation. Therefore, they contribute to the establishment and maintenance of cell contacts. In contrast, pectin epitopes with a low level of de-esterification form matrix gels of low viscosity, allowing cell wall loosening and intercellular space formation. Moreover, these HGA epitopes increase cell wall porosity (Willats *et al.*, 2001; Jarvis *et al.*, 2003; Wolf *et al.*, 2009).

Considering the above, it seems reasonable to suggest that the intensely de-esterified 2F4-HGA epitope in MC contacts contributes to the establishment and maintenance of MC adhesion, while its absence from the wall subdomains of MC isthmus regions correlates with intercellular space formation. The 2F4-HGA epitope may function like the PAM1-HGA epitopes in cell adhesions of dicotyledons (Willats *et al.*, 2001). The 2F4-HGA epitope may complement callose in the establishment and maintenance of cell adhesion at MC contacts, because pectin participation in the cell wall matrix is relatively low in cereals (Carpita, 1996; Fincher, 2009*a*).

The JIM5- and JIM7-HGA epitopes exhibit a relatively low and a very low degree of de-esterification (Knox *et al.*, 1990) respectively, forming matrix cell wall gels of intermediate (JIM5) and very low (JIM7) viscosity. As is the case in dicotyledons (Knox *et al.*, 1990), in nascent and young MCs, the JIM7-HGA epitope resides in the wall regions that will split to create intercellular spaces (Fig. 3C_5, C_6). Its distribution is similar to that of the LM7-HGA epitope in dicotyledons (Willats *et al.*, 2001) and may facilitate intercellular space formation. The co-existence of the JIM7-HGA epitope with the 2F4-HGA epitope in cell contacts of shaping and mature MCs (Fig. 3D_4, D_6, E_4, E_6) may also increase porosity in these cell wall areas, a process promoting communication between adjacent MCs.

As in dicotyledons (Knox *et al.*, 1990), in *Z. mays* the young and shaping MCs of the JIM5-HGA epitope reside at the junctions of cell walls delimiting the forming intercellular spaces (Fig. 7D, E). This pectin may help to define the sites where wall detachment during intercellular space formation will stop. In mature MCs, this epitope is present in the wall thickenings at the cell contacts, which are traversed by plasmodesmata (Fig. 10). Its involvement in primary pit field formation is already known (Casero and Knox, 1995; Orfila and Knox, 2000).

Large quantities of LM6-RGA epitope are detected at the regions of wall detachment during intercellular space formation (Orfila *et al.*, 2001; McCartney and Knox, 2002; Ordaz-Ortiz *et al.*, 2009). The present work confirms the above positional relationship. Since the arabinans are highly flexible and water-soluble polymers (Fry, 2011), it has been suggested that the arabinans linked to RGAs may directly function in cell wall softening or may modulate the HGA properties, facilitating cell wall detachment (Orfila *et al.*, 2001). In differentiating MCs, the LM6-RGA epitope may have a similar function.

Shift in plasmodesmata distribution and formation of plasmodesmata clusters

A combination of primary and secondary plasmodesmata establishes pathways within plant organs whose main functions are the trafficking of nutrients as well as morphogens controlling tissue development. Thus, the cell contacts with their plasmodesmata seem to play crucial roles in these processes (Kragler *et al.*, 1998; Haywood *et al.*, 2002; Xu and Jackson, 2010; Burch-Smith *et al.*, 2011). In *Z. mays* MC initials, an early shift in plasmodesmata distribution is triggered, which results in PC formation in the wall subdomains of the future cell contacts (Figs 5A and 8A, C). Therefore, the above wall subdomains with their plasmodesmata are probably involved in the local entry of MC signals, which coordinate morphogenesis in the entire mesophyll, as is the case with other tissues (Robert and Friml, 2009; Vatén *et al.*, 2011). This is supported by (1) the spatial and temporal co-development of callose patches/PCs between the laterally adjacent MCs and (2) the finding that in many nascent MCs the callose patches are initially established at only one side of the cell (Fig. 4A). In *Z. mays* MCs, the putative morphogenetic signal(s) trigger initially local cell wall differentiation and then microtubule reorganization (see next section). In this process, the PCs should play a crucial role.

Realization of the MC morphogenetic pattern

The present work revealed that MC morphogenesis in cereals is more complex than initially described (Jung and Wernicke, 1990, 1991; Apostolakos *et al.*, 1991; Wernicke and Jung, 1992; Panteris and Galatis, 2005). It reveals the establishment of two distinct structural morphogenetic patterns during MC morphogenesis. The first is created early in MC morphogenesis by the definition of cell contact wall subdomains. The second is created in the cortical cytoplasm by the formation of a definite number of microtubule rings, which define the positions of cell isthmi. Since MC contact determination precedes microtubule ring organization, it may be assumed that the establishment of the first defines or at least affects the position and the number of microtubule rings. The data presented in Table 2 show clearly that each microtubule ring is formed at the mid-region between two successive callose-enriched cell wall bands.

Concerning the mechanism by which the MC contact wall subdomains are involved in the organization of cortical microtubule rings, only assumptions can be made. It has recently been found that in differentiating tracheary elements, the organization of cortical microtubule rings, which defines the pattern of secondary cell wall thickening, is controlled by Rho of Plant (ROP) 11 GTPases. In these cells, distinct microdomains are established in the plasmalemma, where ROP11 GTPases bind preferentially. These, in collaboration with the protein MIcrotubule Depletion Domain (MIDD) 1, induce local disassembly of microtubules in certain areas of cortical cytoplasm and microtubule bundling in others (Oda and Fukuda, 2011, 2012). Considering the similarity in cortical microtubule organization between MCs and tracheary elements, especially the annular ones, it may be supposed that a similar mechanism induces the shift in cortical microtubule organization in MCs from the dispersed type into the grouped type (microtubule rings).

It is also known that a cell wall integrity signalling pathway that induces various cell activities functions in plants. This pathway is based on the production of oligosaccharide fragments of the cell wall, which act as signalling molecules (Fry, 1990) and involves, among other signalling processes, the activation of Rho-like GTPases (reviewed by Wolf *et al.*, 2012). Taking into consideration all the information given in the literature, it can be assumed that the local chemical differentiation of cell wall matrix at MC contact sites may, through a cell wall integrity signalling pathway, define the sites of putative ROP binding to the plasmalemma, which in turn controls the organization of microtubule rings. Therefore, the probable implication of ROP proteins in MC differentiation should be examined.

SUPPLEMENTARY DATA

Supplementary data are available online at www.aob.oxfordjournals.org and consist of the following. Figure S1: area of transverse section of a mature *Zea mays* leaf. Figure S2: shaping MCs as they are seen in DIC optics, and by epifluorescence microscopy under a filter set provided with exciter G365 and barrier LP420 and another with exciter BP450–490 and barrier BP 515–565. Figure S3: TEM micrographs of shaping MCs. Figure S4: young and shaping MCs of *Triticum turgidum* as seen by epifluorescence microscopy after aniline blue staining. Figure S5: immunodetection of cell wall matrix polysaccharides in sections of nascent MCs embedded in LRW. Video: nascent MCs after callose immunolocalization. The callose-enriched cell wall bands and their opposite arrangement in adjacent MCs can be easily observed.

ACKNOWLEDGEMENTS

The authors greatly acknowledge Dr Nigel Chaffey and the reviewers for critical reading of the manuscript and their helpful comments, which contributed to the better presentation of the present work, and to Dr K. Karpouzis for the preparation of the video material.

LITERATURE CITED

Apostolakos P, Galatis B, Panteris E. 1991. Microtubules in cell morphogenesis and intercellular space formation in *Zea mays* leaf mesophyll and *Pilea cadierei* epithem. *Journal of Plant Physiology* **137**: 591–601.

Apostolakos P, Livanos P, Nikolakopoulou TL, Galatis B. 2009. The role of callose in guard cell wall differentiation and stomatal pore formation in the fern *Asplenium nidus* L. *Annals of Botany* **104**: 1373–1387.

Basic A, Fincher GB, Stone BA. 2009. *Chemistry, biochemistry, and biology of (1→3)-β-glucans and related polysaccharides.* Amsterdam: Academic Press.

Buckeridge MS, Rayon C, Urbanowicz B, Tine MAS, Carpita N. 2004. Mixed linkage (1→3)(1→4)-β-D-glucans of grasses. *Cereal Chemistry* **81**: 115–127.

Burch-Smith TM, Brunkard OJ, Choi YG, Zambruski PC. 2011. Organelle-nucleus cross talk regulates plant intercellular communication via plasmodesmata. *Proceedings of the National Academy of Science, USA* **108**: E1451–E1460.

Burton RA, Fincher GB. 2009. (1,3; 1,4)-β-D-glucans in cell walls of the Poaceae, lower plants, and fungi: a tale of two linkages. *Molecular Plant* **2**: 873–882.

Carpita NC. 1996. Structure and biogenesis of the cell walls of grasses. *Annual Review of Plant Physiology and Plant Molecular Biology* **47**: 445–476.

Carpita NC, Defernez M, Findlay K, *et al*. 2001. Cell wall architecture of the elongating maize coleoptile. *Plant Physiology* **127**: 551–565.

Casero PJ, Knox JP. 1995. The monoclonal antibody JIM5 indicates patterns of pectin deposition in relation to pit fields at the plasma-membrane-face of tomato pericarp cell walls. *Protoplasma* **188**: 133–137.

Chen XY, Kim JY. 2009. Callose synthesis in higher plants. *Plant Signaling and Behavior* **4**: 489–492.

Douchiche O, Driouich A, Morvan C. 2010. Spatial regulation of cell-wall structure in response to heavy metal stress: cadmium-induced alteration of the methyl-esterification pattern of homogalacturonans. *Annals of Botany* **105**: 481–491.

Eder M, Lütz-Meindl U. 2010. Analyses and localization of pectin-like carbohydrates in cell wall and mucilage of the green alga *Netrium digitus*. *Protoplasma* **243**: 25–38.

Ehlers K, Kollmann R. 2001. Primary and secondary plasmodesmata: structure, origin and functioning. *Protoplasma* **216**: 1–30.

Evert RF, Eschrich W, Heyser W. 1977. Distribution and structure of plasmodesmata in mesophyll and bundle-sheath cells of *Zea mays* L. *Planta* **136**: 77–89.

Faulkner C, Akman OE, Bell K, Jeffree C, Oparka K. 2008. Peeking into pit fields: a multiple twinning model of secondary plasmodesmata formation in tobacco. *Plant Cell* **20**: 1504–1518.

Fincher GB. 2009*a*. Revolutionary times in our understanding of cell wall biosynthesis and remodeling in the grasses. *Plant Physiology* **149**: 27–37.

Fincher GB. 2009*b*. Exploring the evolution of (1→3) (1→4)-β-D-glucans in plant cell walls: comparative genomics can help! *Current Opinion in Plant Biology* **12**: 140–147.

Fry SC. 1990. Roles of the primary cell wall in morphogenesis. In: Nijkamp HJJ, van der Plas LHW, van Aartrijk J. eds. *Progress in plant cellular and molecular biology*. Dordrecht: Kluwer, 504–513.

Fry SC. 2011. Cell wall polysaccharide composition and covalent crosslinking. *Annual Plant Reviews* **41**: 1–42.

Fry SC, Nesselrode BHW, Miller JG, Newburn BR. 2008. Mixed-linkage of (1→3) (1→4)-β-D-glucan is a major hemicellulose of *Equisetum* (horsetail) cell walls. *New Phytologist* **179**: 104–115.

Galatis B. 1988. Morphogenesis of the epithem cells in hydathodes of *Pilea cadierei*. *Planta* **176**: 287–297.

Galatis B, Apostolakos P. 2010. A new callose function. Involvement in differentiation and function of fern stomatal complexes. *Plant Signaling and Behavior* **5**: 1359–1364.

Giannoutsou E, Apostolakos P, Galatis B. 2011. Actin filament-organized local cortical endoplasmic reticulum aggregations in developing stomatal complexes of grasses. *Protoplasma* **248**: 373–390.

Haywood V, Kragler F, Lucas WJ. 2002. Plasmodesmata: pathways for protein and ribonucleoprotein signaling. *Plant Cell Supplement* **2002**: S303–S325.

Hervé C, Rogowski A, Gilbert HJ, Knox JP. 2009. Enzymatic treatments reveal differential capacities of xylan recognition and degradation in primary and secondary plant cell walls. *Plant Journal* **58**: 413–422.

Heslop-Harrison J. 1964. Cell walls, cell membranes and protoplasmic connections during meiosis and pollen development. In: Linskens HF. ed. *Pollen physiology and fertilization*. Amsterdam: North-Holland, 29–47.

Jarvis MC, Briggs SPH, Knox JP. 2003. Intercellular adhesion and cell separation in plants. *Plant Cell and Environment* **26**: 977–989.

Jung G, Wernicke W. 1990. Cell shaping and microtubules in developing mesophyll of wheat (*Triticum aestivum* L.). *Protoplasma* **153**: 141–148.

Jung G, Wernicke W. 1991. Patterns of actin filaments during cell shaping in developing mesophyll of wheat (*Triticum aestivum* L.). *European Journal of Cell Biology* **56**: 139–146.

Knox JP. 1992. Cell-adhesion, cell-separation and plant morphogenesis. *Plant Journal* **2**: 137–141.

Knox JP, Linstead PJ, King J, Cooper C, Roberts K. 1990. Pectin esterification is spatially regulated both within cell walls and between developing tissues of root apices. *Planta* **181**: 512–521.

Kragler F, Lucas WJ, Monzer J. 1998. Plasmodesmata: dynamics, domains and patterning. *Annals of Botany* **81**: 1–10.

Lee KJD, Marcus SE, Knox JP. 2011. Cell wall biology: perspectives from cell wall imaging. *Molecular Plant* **4**: 212–219.

Liners F, Letesson JJ, Didembourg C, Van Cutsem P. 1989. Monoclonal antibodies against pectin. Recognition of conformation induced by calcium. *Plant Physiology* **91**: 1419–1424.

Marcus SE, Verhertbruggen Y, Hervé C, *et al*. 2008. Pectic homogalacturonan masks abundant sets of xyloglucan epitopes in plant cell walls. *BMC Plant Biology* **8**: 60.

Marcus SE, Blake AW, Benians TA, *et al*. 2010. Restricted access of proteins to mannan polysaccharides in intact plant cell walls. *Plant Journal* **64**: 191–203.

Mauseth JD. 1988. *Plant anatomy*. Redwood City, CA: Benjamin/Cummings.

Mauseth JD. 1998. *Botany. An introduction to plant biology* Boston, MA: Jones and Bartlett.

McCartney L, Knox JP. 2002. Regulation of pectic polysaccharide domains in relation to cell development and cell properties in the pea testa. *Journal of Experimental Botany* **53**: 707–714.

Metcalfe CR. 1960. *Anatomy of the monocotyledons I. Gramineae*. London: Oxford University Press.

Michelli F. 2001. Pectin methylesterases: cell wall enzymes with important roles in plant physiology. *Trends in Plant Science* **6**: 414–419.

O'Brien TP, McCully ME. 1981. *The study of plant structure: principles and selected methods*. Melbourne: Termarcarphi.

Oda Y, Fukuda H. 2011. Secondary cell wall patterning during xylem differentiation. *Current Opinion in Plant Biology* **15**: 1–7.

Oda Y, Fukuda H. 2012. Initiation of cell wall pattern by a Rho- and microtubule-driven symmetry breaking. *Science* **337**: 1333–1336.

Ordaz-Ortiz JJ, Marcus SE, Knox JP. 2009. Cell wall microstructure analysis implicates hemicellulose polysaccharides in cell adhesion in tomato fruit pericarp parenchyma. *Molecular Plant* **2**: 910–921.

Orfila C, Knox JP. 2000. Spatial regulation of pectic polysaccharides in relation to pit fields in cell walls of tomato fruit pericarp. *Plant Physiology* **122**: 775–781.

Orfila C, Seymour GB, Willats WGT, *et al*. 2001. Altered middle lamella homogalacturonan and disrupted deposition of (1→5)-alpha-L-arabinan in the pericarp of *Cnr,* a ripening mutant of tomato. *Plant Physiology* **126**: 210–221.

Panteris E, Galatis B. 2005. The morphogenesis of lobed plant cells in the mesophyll and epidermis: organization and distinct roles of cortical microtubules and actin filaments. *New Phytologist* **67**: 721–732.

Panteris E, Apostolakos P, Galatis B. 1993*a*. Microtubule organization, mesophyll cell morphogenesis, and intercellular space formation in *Adiantum capillus-veneris* leaflets. *Protoplasma* **172**: 97–110.

Panteris E, Apostolakos P, Galatis B. 1993*b*. Microtubule organization and cell morphogenesis in two semi-lobed cell types of *Adiantum capillus-veneris* L. leaflets. *New Phytologist* **125**: 509–520.

Parre E, Geitmann A. 2005. More than a leak sealant. The mechanical properties of callose in pollen tubes. *Plant Physiology* **37**: 274–286.

Piršelová B, Matušíková I. 2012. Callose: the plant cell wall polysaccharide with multiple biological functions. *Acta Physiologiae Plantarum* **35**: 635–644.

Ridley BL, O'Neill MA, Mohnen D. 2001. Pectins: structure, biosynthesis, and oligogalacturonide-related signaling. *Phytochemistry* **57**: 929–967.

Robert HS, Friml J. 2009. Auxin and other signals on the move in plants. *Nature Chemical Biology* **5**: 325–332.

Stone BA, Clarke AE. 1992. *Chemistry and biology of* (*1→3*)-β-*glucans.* Bundora, Australia: La Trobe University Press.

VandenBosch KA, Bradley DJ, Knox JP, Perotto S, Butcher GW, Brewin NJ. 1989. Common components of the infection thread matrix and the intercellular space identified by immunocytochemical analysis of pea nodules and uninfected roots. *EMBO Journal* **8**: 335–342.

Vatén A, Dettmer J, Wu S, Stierhof YD, *et al*. 2011. Callose biosynthesis regulates symplastic trafficking during root development. *Developmental Cell* **21**: 1144–1155.

Vaughn KC, Talbot MJ, Offler CE, McCurdy DW. 2007. Wall ingrowths in epidermal transfer cells of *Vicia faba* cotelydons are modified primary walls marked by localized accumulations of arabinogalactan proteins. *Plant and Cell Physiology* **48**: 159–168.

Wang H-T, Liu I-H, Yeh T-F. 2012. Immunohistological study of mannan polysaccharides in poplar stem. *Cellulose Chemistry and Technology* **46**: 149–155.

Wernicke W, Jung G. 1992. Role of cytoskeleton in cell shaping of developing mesophyll of wheat (*Triticum aestivum* L.). *European Journal of Cell Biology* **57**: 88–94.

Wernicke W, Gunther P, Jung G. 1993. Microtubules and cell shaping in the mesophyll of *Nigella damascena* L. Protoplasm*a* **173**: 8–12.

Willats WGT, Marcus SE, Knox JP. 1998. Generation of a monoclonal antibody specific to (1→5)-alpha-L-arabinan. *Carbohydrate Research* **308**: 149–152.

Willats WG, McCartney L, Mackie W, Knox JP. 2001. Pectin: cell biology and prospects for functional analysis. *Plant Molecular Biology* **47**: 9–27.

Willats WGT, McCartneySteele-King CG, *et al*. 2004. A xylogalacturonan epitope is specifically associated with plant cell detachment. *Planta* **218**: 673–681.

Wolf S, Mouille G, Pelloux J. 2009. Homogalacturonan, methyl-esterification and plant development. *Molecular Plant* **2**: 851–860.

Wolf S, Hématy K, Höfte H. 2012. Growth control and cell wall signaling in plants. *Annual Review of Plant Biology* **63**: 381–407.

Xu X, Jackson D. 2010. Lights at the end of the tunnel: new views of plasmodesmal structure and function. *Current Opinion in Plant Biology* **13**: 684–692.